

~~CONFIDENTIAL~~

Copy 386  
RM L58C19

NACA

# RESEARCH MEMORANDUM

Declassified by authority of NASA  
Classification Change Notices No. 43  
Dated \*\*12/22/65

INVESTIGATION OF CONTROL EFFECTIVENESS AND STABILITY  
CHARACTERISTICS OF A MODEL OF A LOW-WING MISSILE  
WITH INTERDIGITATED TAIL SURFACES AT MACH  
NUMBERS OF 2.29, 2.97, AND 3.51

By John G. Presnell, Jr.

Langley Aeronautical Laboratory  
Langley Field, Va.

DECLASSIFIED:  
ATS 480

AUTHORITY:  
DROBKA TO LEBOW  
MEMO DATED 12/13/65

~~CONFIDENTIAL~~

NATIONAL ADVISORY COMMITTEE  
FOR AERONAUTICS

WASHINGTON

July 14, 1958

~~CONFIDENTIAL~~

CONFIDENTIAL  
NATIONAL ADVISORY COMMITTEE FOR AERONAUTICS

RESEARCH MEMORANDUM

INVESTIGATION OF CONTROL EFFECTIVENESS AND STABILITY

CHARACTERISTICS OF A MODEL OF A LOW-WING MISSILE

WITH INTERDIGITATED TAIL SURFACES AT MACH

NUMBERS OF 2.29, 2.97, AND 3.51\*

By John G. Presnell, Jr.

SUMMARY

A brief investigation of the longitudinal stability and control effectiveness at supersonic speeds of a model of a low-wing missile with interdigitated tail surfaces was made in the Langley Unitary Plan wind tunnel. The data were obtained at Mach numbers  $M$  of 2.29, 2.97, and 3.51 for Reynolds numbers (based on the mean geometric chord of the wing) of  $1.15 \times 10^6$ ,  $1.14 \times 10^6$ , and  $1.11 \times 10^6$ , respectively. Data were obtained for three settings of the longitudinal control surfaces: with deflection of all surfaces, with deflection of the lower surfaces only, and with all surfaces undeflected. Directional stability data were obtained at  $M = 3.51$  for angles of attack of approximately  $0^\circ$  and  $10^\circ$ . These data, with summary data and typical schlieren photographs, are presented with only a brief analysis.

The data indicate that the controls are effective throughout the Mach number range and lift-coefficient range ( $C_L = -0.15$  to  $0.7$ , approximately) of the tests. There is a severe break in the pitching-moment curve at  $M = 2.29$  which might result in a pitch-up condition in flight, and also a large forward movement of the aerodynamic center with increasing Mach number that produces neutral longitudinal stability at  $M = 3.51$  for the moment center used in this investigation. The model was directionally unstable at  $M = 3.51$ ; however, the level of directional stability was about the same for  $0^\circ$  and  $10^\circ$  angles of attack.

INTRODUCTION

The problem of aerodynamic control of an air-launched missile that is to be carried externally and yet is large enough to attack and destroy

---

\*Title, Unclassified.

primary sea targets and permanent land installations is quite difficult because the size of the control surfaces, if they do not fold, is limited by the available carriage space under the mother aircraft. Use is made of interdigitated tail surfaces since they require less space in the vertical and horizontal planes than conventional vertical and horizontal tails with the same surface area.

An investigation of the longitudinal control effectiveness of a model of a low-wing missile with interdigitated or cruciform tail surfaces was made in the Langley Unitary Plan wind tunnel at Mach numbers of 2.29, 2.97, and 3.51.

The results of the investigation are presented herein with a brief evaluation of the drag and longitudinal and lateral stability characteristics of the model.

### SYMBOLS

The stability system of axes to which the results are referenced and the positive directions of angles, forces, and moments are shown in figure 1. The deflection of the control surfaces is positive with the trailing edge of each panel down. Moment coefficients are referred to the point located at the 0.25 station of the mean geometric chord of the wing (moment center shown in fig. 2).

b	wing span, in.
$\bar{c}$	wing mean geometric chord, in.
$C_L$	lift coefficient, $Lift/qS$
$C_l$	rolling-moment coefficient, $\frac{\text{Rolling moment}}{qSb}$
$C_D$	drag coefficient, $Drag/qS$
$C_{D_b}$	base drag coefficient on model
$C_m$	pitching-moment coefficient, $\frac{\text{Pitching moment}}{qS\bar{c}}$
$C_n$	yawing-moment coefficient, $\frac{\text{Yawing moment}}{qSb}$

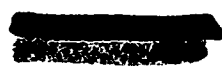
$C_Y$	side-force coefficient, $\frac{\text{Side force}}{qS}$
$C_{L_\alpha}$	lift-curve slope ( $\beta = 0^\circ$ ), $\frac{\partial C_L}{\partial \alpha}$
$C_{m_{C_L}}$	pitching-moment-curve slope ( $C_L = 0^\circ$ ), $\frac{\partial C_m}{\partial C_L}$
$C_{m_\delta}$	longitudinal control-surface effectiveness, $\frac{\partial C_m}{\partial \delta}$
$L/D$	lift-drag ratio, $C_L/C_D$
$M$	free-stream Mach number
$q$	free-stream dynamic pressure, lb/sq ft
$S$	wing area including body intercept, sq ft
$X, Y, Z$	stability axes (see fig. 1)
$\alpha$	angle of attack referred to fuselage reference line, deg
$\beta$	angle of sideslip referred to fuselage center line, deg
$\delta$	control-panel deflection about control-surface hinge line, deg (fig. 2, view A-A)

## Subscripts:

$l$	lower two control surfaces of interdigitated tail
$u$	upper two control surfaces of interdigitated tail
$0$	value at zero lift condition
$\text{max}$	maximum
$\text{min}$	minimum

## APPARATUS AND MODEL

The tests were conducted in the high Mach number test section of the Langley Unitary Plan wind tunnel which is a variable-pressure,





0371320130

CONFIDENTIAL

NACA RM L58C19

continuous, return-flow type. The test section is 4 feet square and approximately 7 feet in length. The nozzle leading to the test section is of the asymmetric sliding-block type and the Mach number may be varied through a range from approximately  $M = 2.29$  to  $M = 4.65$  without tunnel shutdown. Forces and moments on the model were measured by means of a six-component internal strain-gage balance. This balance was attached by means of a sting to the model support system. Included in this support system was remotely operated, adjustable-angle coupling that permitted tests to be made at variable angles of attack concurrently with variations in the angle of sideslip.

Details of the model are shown in figure 2 and its geometric characteristics are given in table I. Photographs of the model are presented as figure 3. The model has a low wing with an aspect ratio of 1.78, an NACA 0004 airfoil section, and a leading-edge sweepback of  $62.1^\circ$ . The fuselage is a body of revolution with a relatively high degree of boattailing.

The interdigitated tail surfaces consist of four identical panels with modified double-wedge 4-percent-thick airfoil sections, having a total area of 0.206 square foot and an effective tail length from the quarter-chord of the wing mean geometric chord to the quarter-chord of the tail mean geometric chord of 12.184 inches. Positive deflection of these panels is with trailing edge down.

#### TESTS

Tests were made through an angle-of-attack range from approximately  $-4^\circ$  to  $21^\circ$  at  $0^\circ$  angle of sideslip for Mach numbers of 2.29, 2.97, and 3.51, with the control surfaces undeflected, with  $-5^\circ$  deflection on all surfaces, and with only the lower surfaces deflected  $-5^\circ$ . For  $M = 3.51$  tests were also made through an angle-of-sideslip range from approximately  $-10^\circ$  to  $10^\circ$  at approximately  $0^\circ$  and  $10^\circ$  angles of attack.

Test conditions of Mach number, stagnation and dynamic pressures, and Reynolds number (based on the mean geometric chord of the wing) are listed in the following table:

Mach number, M	Stagnation pressure, lb/sq in. abs	Dynamic pressure, lb/sq ft	Reynolds number
2.29	9.6	412	$1.15 \times 10^6$
2.97	13.5	342	1.14
3.51	17.4	279	1.11

The dewpoint for all tests was maintained below  $-30^{\circ}$  F to prevent adverse condensation effects. The stagnation temperature was maintained at  $150^{\circ}$  F.

#### CORRECTIONS AND ACCURACY

The tunnel, as yet, has not been completely calibrated but preliminary findings of the flow-angularity calibration indicate that the model experiences upflow of about  $0.35^{\circ}$  at  $M = 2.29$ ,  $0.20^{\circ}$  at  $M = 2.97$ , and  $0.10^{\circ}$  at  $M = 3.51$ . The angularity corrections are not included in the results presented herein and should be considered in evaluations of the drag results and the angle of attack for zero lift conditions. Pressure gradients in the region of the model have been determined and are sufficiently small to induce negligible buoyancy on the model.

The maximum deviation of local Mach number in the portion of the tunnel occupied by the model was  $\pm 0.015$  from the average values listed in the preceding section.

The angles of attack and sideslip have been corrected for deflection of the balance-sting combination under load. The control-surface deflection angles have not been corrected for surface loads.

The base drag of the model was obtained for all test points and has been subtracted from the measured total drag. The drag results presented herein have, therefore, been corrected to conditions of free-stream static pressure at the model base.

The estimated accuracy of the force and moment coefficients, based on balance calibration and repeatability of the data, is within the following limits:

$C_L$	$\pm 0.002$
$C_D$	$\pm 0.0010$
$C_m$	$\pm 0.001$
$C_n$	$\pm 0.0005$
$C_Y$	$\pm 0.0015$

## PRESENTATION OF RESULTS

The results of the investigation are presented in the following figures:

	Figure
Schlieren photographs of the test model . . . . .	4
Variation of base drag coefficient with angle of attack . . . . .	5
Pitch characteristics of the test model . . . . .	6
Summary of pitch characteristics of the test model . . . . .	7
Control effectiveness of the test model . . . . .	8
Lateral characteristics of the test model at $M = 3.51$ . . . . .	9


The lateral coefficients presented do not include the rolling-moment coefficients because they were not considered valid owing to mechanical malfunction of the balance during the test.

## DISCUSSION

The data indicated that the interdigitated tail surfaces have control effectiveness  $C_{m\delta}$  throughout the Mach number range ( $M = 2.29$  to  $3.51$ ) and lift-coefficient range ( $C_L = -0.15$  to  $0.7$ , approximately) of the tests. With increasing lift coefficient, the lower surfaces gain effectiveness while the upper surfaces lose effectiveness, as would be expected. For an increase in lift coefficient from  $0$  to  $0.5$ , the complete tail exhibits an increase in effectiveness of about  $0.001$  over the Mach number range while the lower surfaces alone exhibit an increase varying from  $0.0015$  at  $M = 2.29$  to  $0.0028$  at  $M = 3.51$ . This leads to the conclusion that with increasing Mach number the rate of loss in effectiveness of the upper surfaces is offset by an almost equal rate of gain in effectiveness of the lower surfaces (fig. 8).

The pitch data have two other main points of interest. One of these is a severe break in the pitching-moment curve at  $M = 2.29$  which might result in a pitchup condition in flight. This condition seems to be reduced with increasing Mach number (fig. 7). The other is a very large forward movement of the aerodynamic center with increase in Mach number ( $0.19\bar{c}$  from  $M = 2.29$  to  $M = 3.51$ ) that produces neutral longitudinal stability at  $M = 3.51$  for the moment center used in this investigation.

The lateral data, taken at  $M = 3.51$  only, show that the model is directionally unstable (fig. 9). These data also show that angle of attack has very little effect on the lateral characteristics.



CONFIDENTIAL

## CONCLUSIONS

An investigation of a model of a low-wing missile with interdigitated tail surfaces to determine the control effectiveness and stability characteristics has been made at Mach numbers of 2.29, 2.97, and 3.51. The results indicated the following conclusions:

1. The tail surfaces have control effectiveness over the Mach number range of the tests ( $M = 2.29$  to  $3.51$ ). The lower surfaces contribute a large part of the effectiveness at the higher lift coefficient.

2. The pitch data show a severe break in the pitching-moment curve at  $M = 2.29$ , which might result in a pitch-up condition in flight, and also show a very large forward movement of the aerodynamic center with increasing Mach number, which produces neutral longitudinal stability at  $M = 3.51$  for the moment center used in this investigation.

3. The model is directionally unstable at  $M = 3.51$ . The level of directional instability is affected very little by an increase of  $10^\circ$  in angle of attack.

Langley Aeronautical Laboratory,  
National Advisory Committee for Aeronautics,  
Langley Field, Va., February 28, 1958.




TABLE I.- PHYSICAL CHARACTERISTICS OF THE MODEL OF A LOW-WING  
MISSILE WITH INTERDIGITATED TAIL SURFACES

## Body:

Length, in. . . . .	34.56
Maximum diameter, in. . . . .	3.42
Moment center (on body center line), distance from nose, in. . . . .	17.513
Base area, sq ft . . . . .	0.0101

## Wing:

Area, sq ft . . . . .	0.466
Span, ft . . . . .	0.90
Root chord, in. . . . .	11.311
Tip chord, in. . . . .	1.131
Taper ratio . . . . .	0.10
Aspect ratio (theoretical) . . . . .	1.738
Mean geometric chord, in. . . . .	7.609
Leading edge of M.G.C., distance from nose, in. . . . .	15.611
Airfoil section . . . . .	NACA 0004
Sweepback of leading edge, deg . . . . .	62.053
Sweepback of quarter-chord line, deg . . . . .	54.7
Incidence, deg . . . . .	0
Dihedral, deg . . . . .	0

## Tail surfaces:

Area, each panel, sq ft . . . . .	0.0515
Area, total, sq ft . . . . .	0.206
Root chord, in. . . . .	3.875
Tip chord, in. . . . .	0.457
Taper ratio . . . . .	0.118
Aspect ratio (theoretical, each panel) . . . . .	1.577
Mean geometric chord, in. . . . .	2.608
Leading edge of M.G.C. of tail, distance from nose, in. . . . .	29.045
Moment arm of tail, quarter-chord of wing M.G.C. to quarter-chord of tail M.G.C., in. . . . .	12.184
Tail-surface hinge line, distance from nose, in. . . . .	30.420
Airfoil section . . . . .	Modified double-wedge 4% thick

CONFIDENTIAL

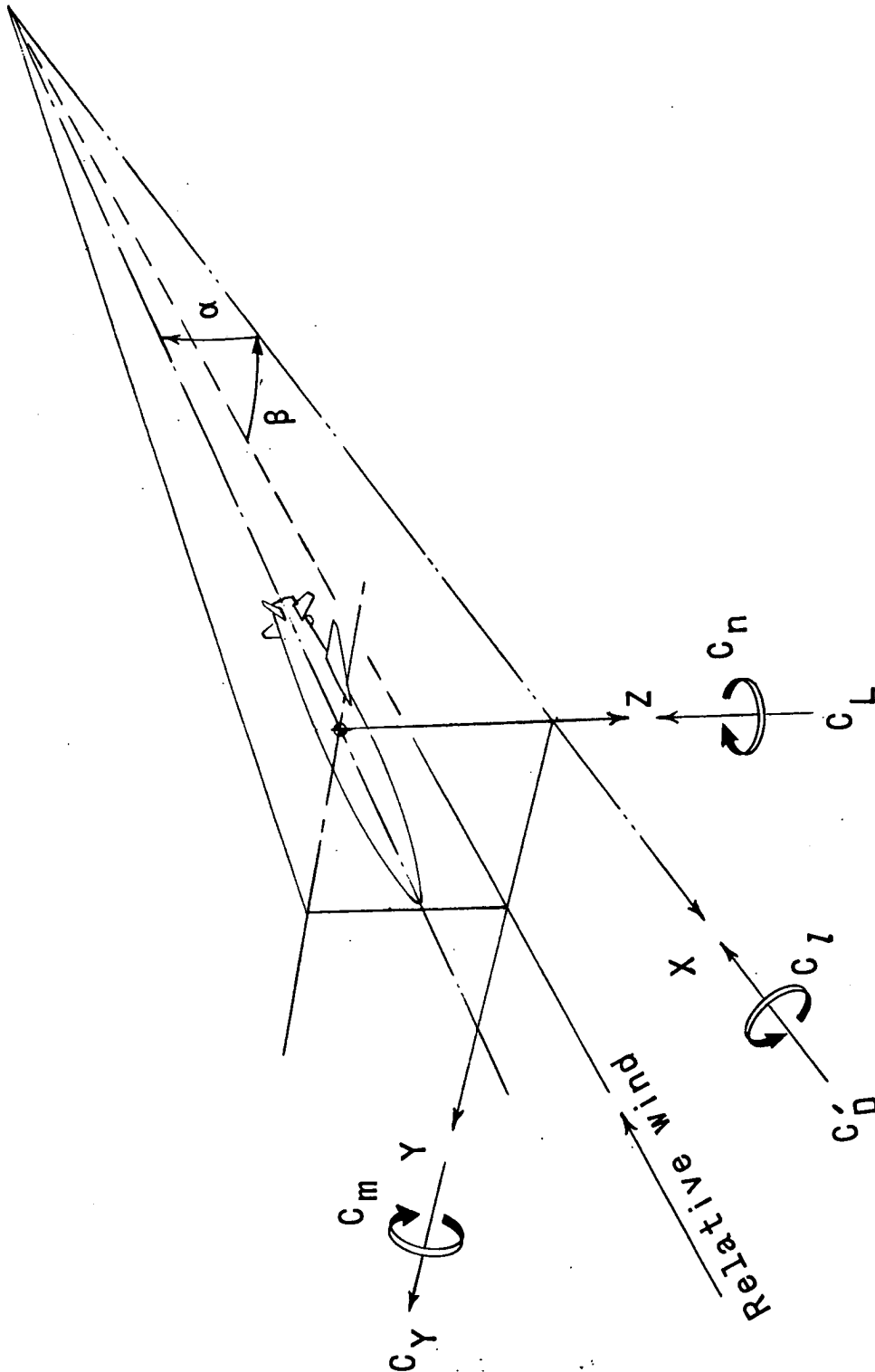


Figure 1.- Stability system of axes. Arrows indicate positive directions of angles, forces, and moments.

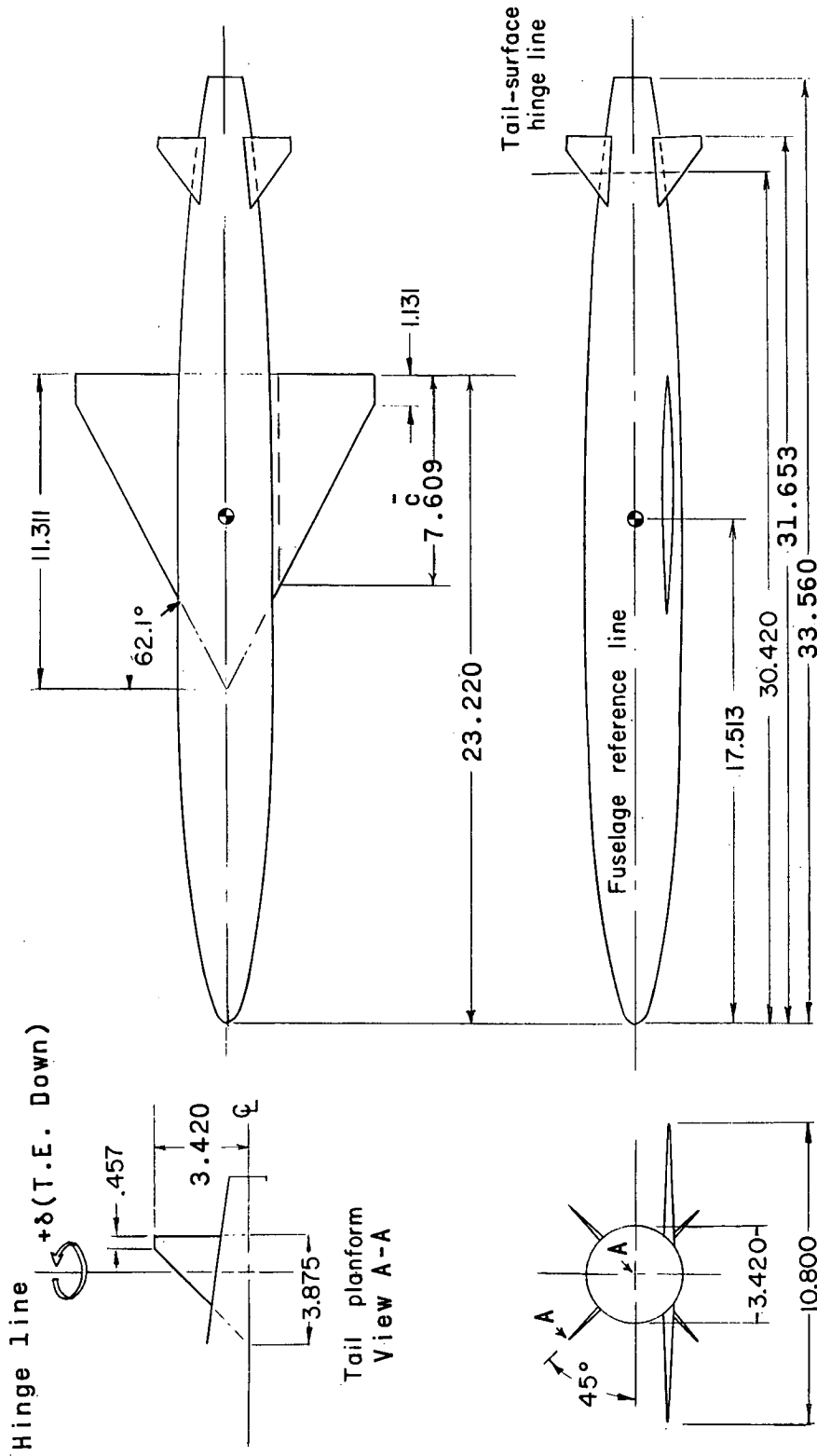
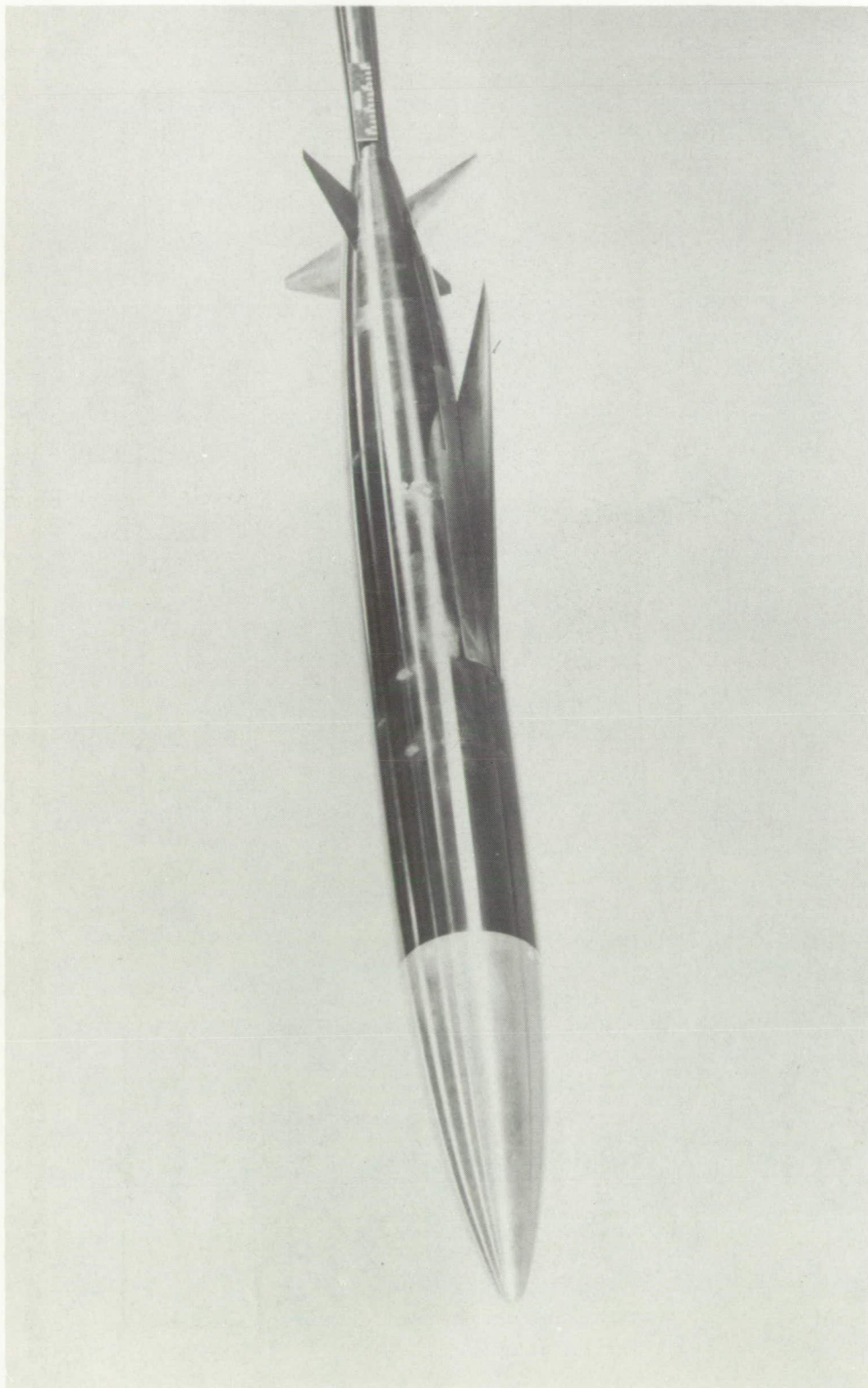


Figure 2.- Details of a low-wing missile with interdigitated tail surfaces. All dimensions are in inches unless otherwise noted.



DECLASSIFIED  
CONFIDENTIAL



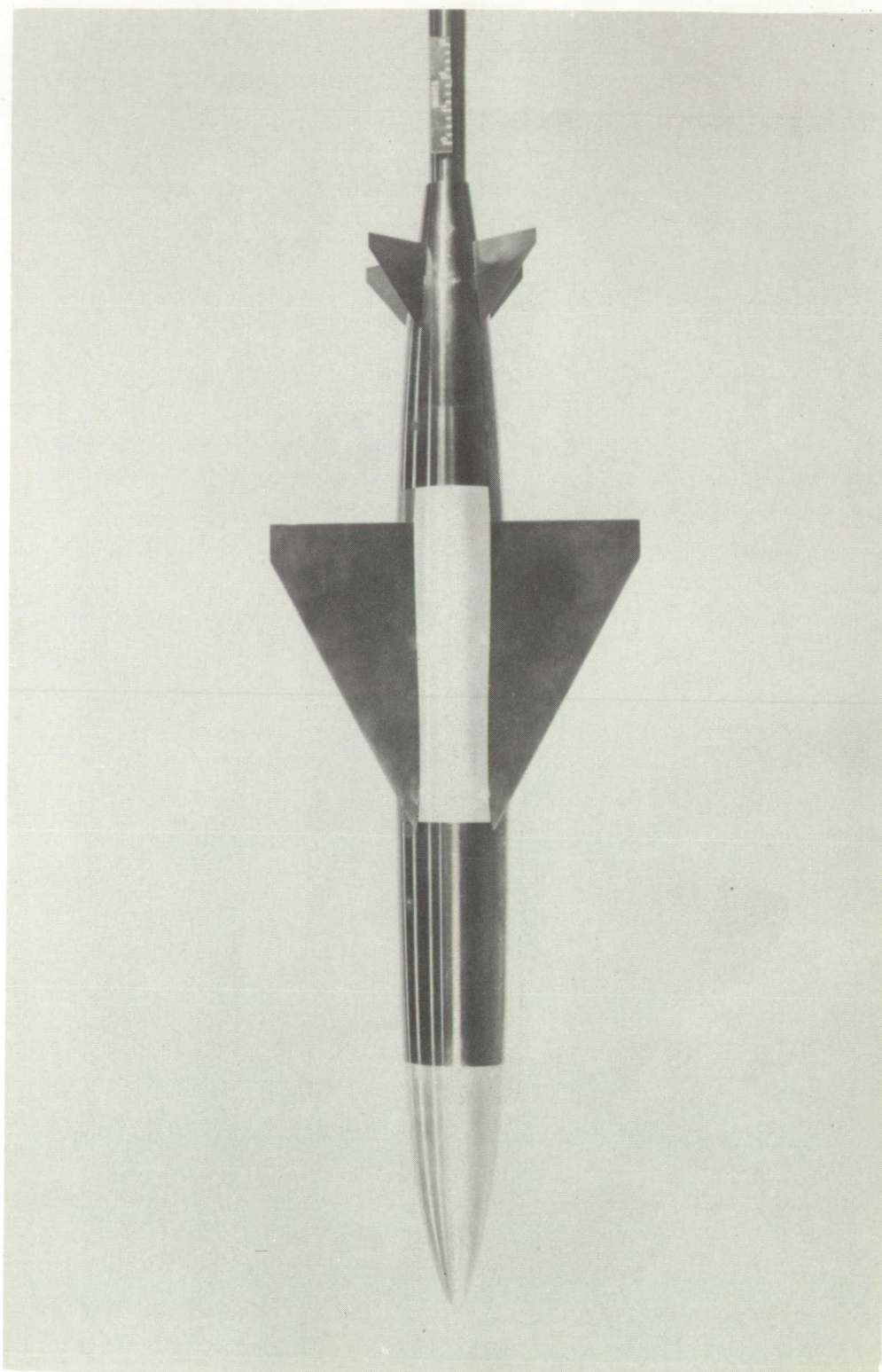
L-57-1489

Figure 3.- Low-wing missile with interdigitated tail surfaces.

03710301030

CONFIDENTIAL

NACA RM L58C19



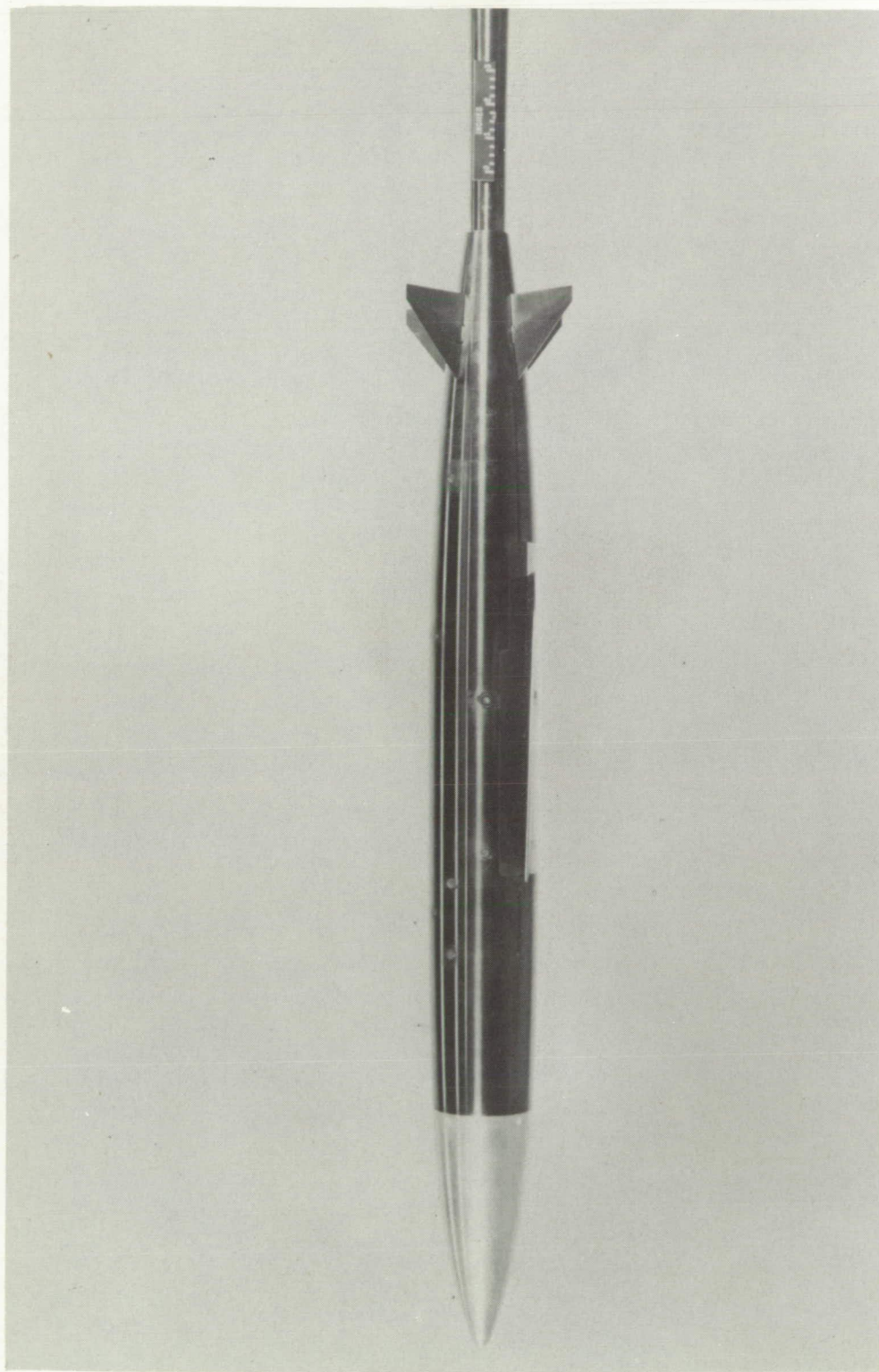
L-57-1488

Figure 3.- Continued.

CONFIDENTIAL



CONFIDENTIAL



I-57-1486

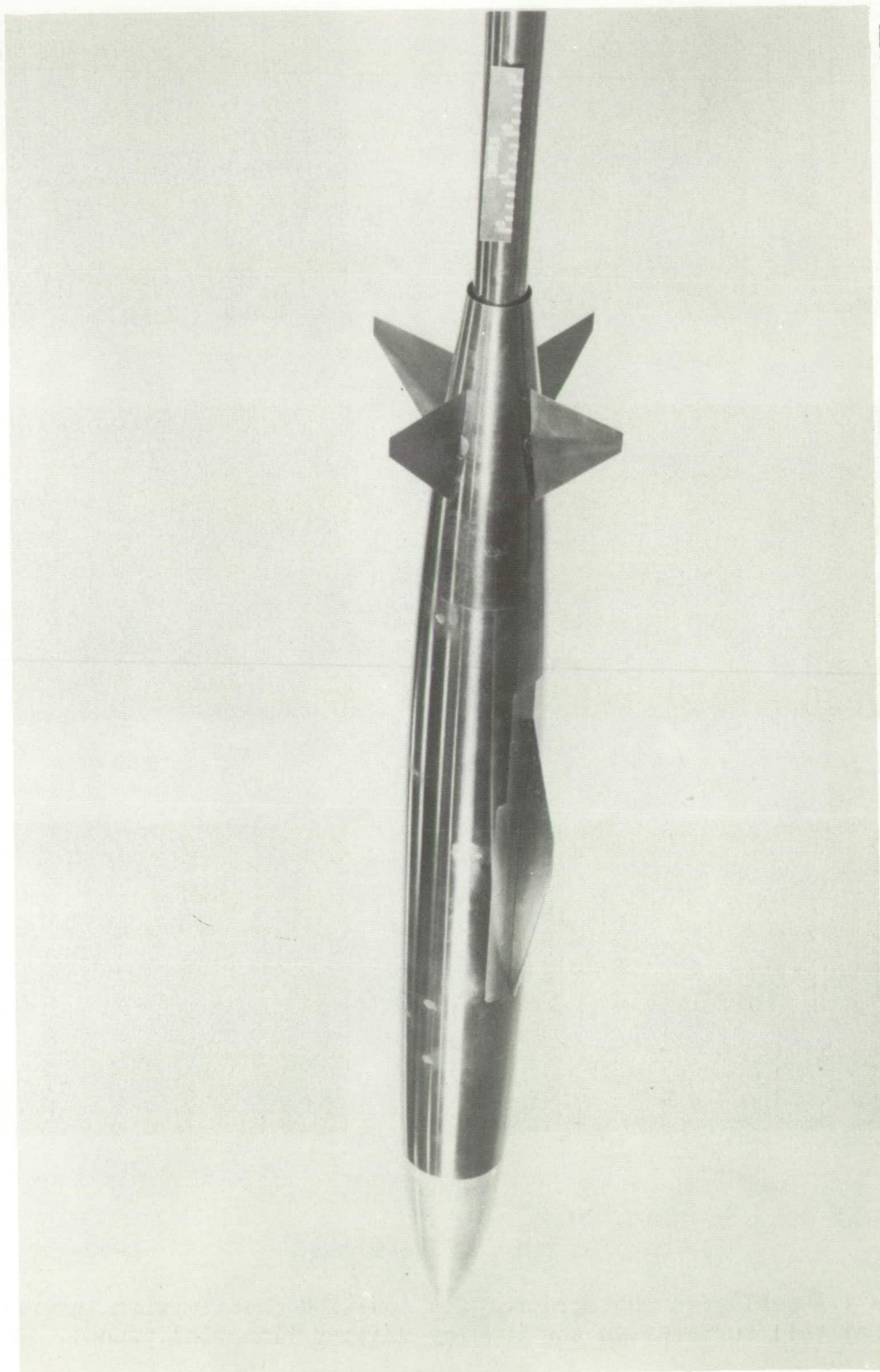
Figure 3.- Continued.

CONFIDENTIAL

031712201030

CONFIDENTIAL

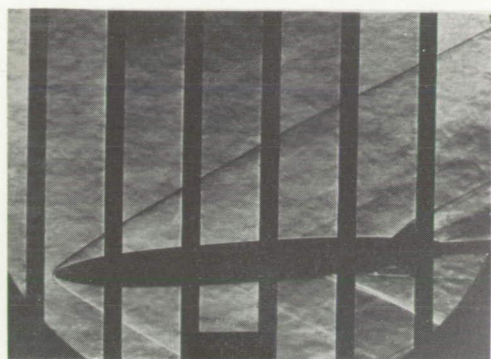
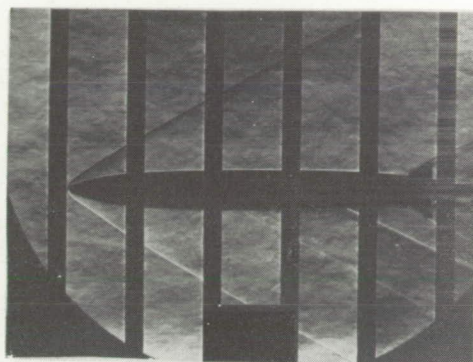
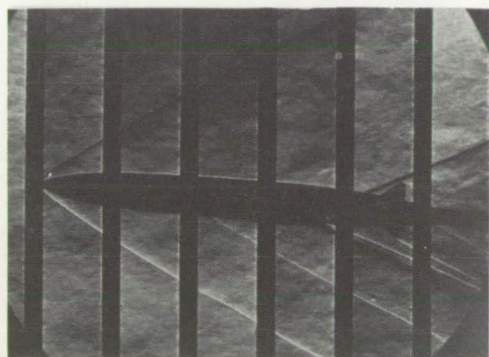
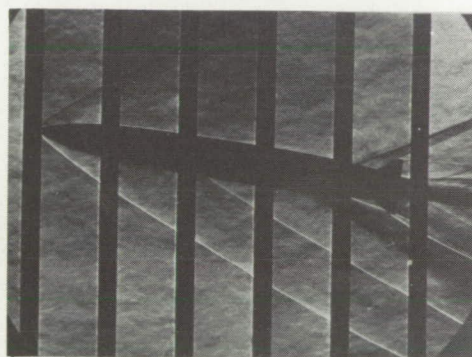
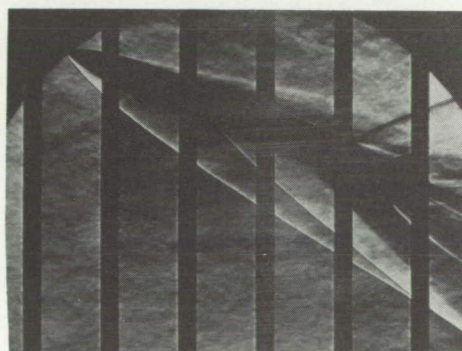
NACA RM L58C19



L-57-1487

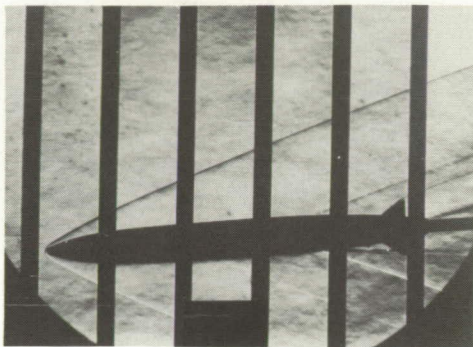
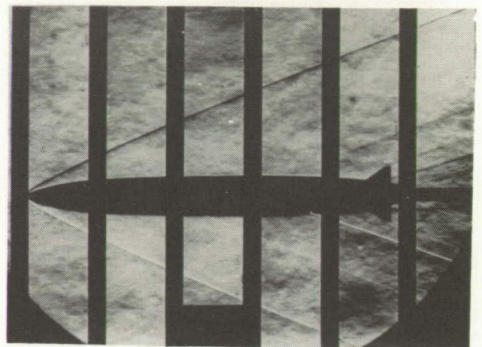
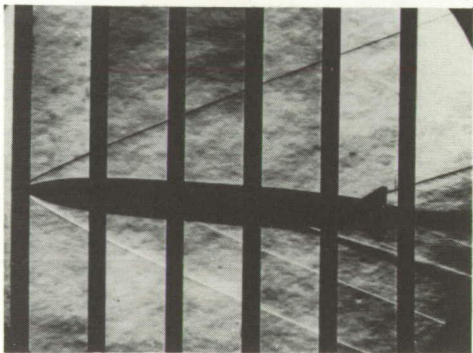
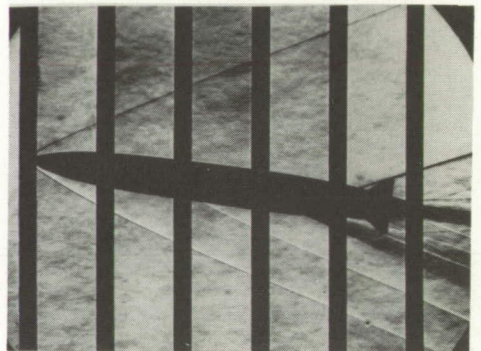
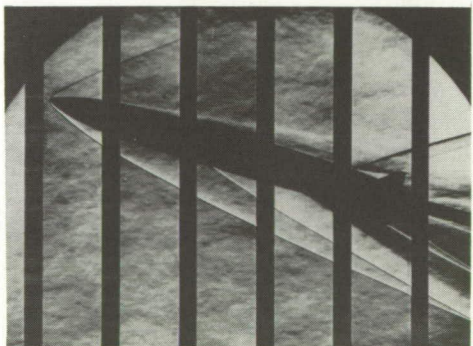
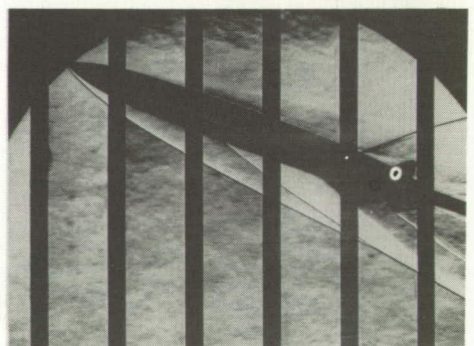
Figure 3.- Concluded.



 $\alpha = -4.1^\circ$  $\alpha = 0^\circ$  $\alpha = 4.2^\circ$  $\alpha = 8.4^\circ$  $\alpha = 17.2^\circ$  $\alpha = 21.5^\circ$ (a)  $M = 2.29$ .

L-58-158

Figure 4.- Schlieren photographs of a low-wing missile with interdigitated tail surfaces in the Langley Unitary Plan wind tunnel.  $\beta = 0^\circ$ .

 $\alpha = -4.1^\circ$  $\alpha = 0^\circ$  $\alpha = 4.1^\circ$  $\alpha = 8.2^\circ$  $\alpha = 16.8^\circ$  $\alpha = 21.0^\circ$ (b)  $M = 2.97$ .

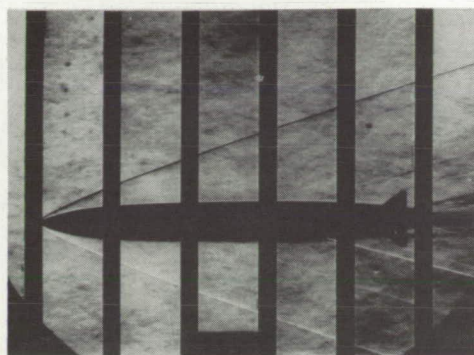
L-58-159

Figure 4.- Continued.

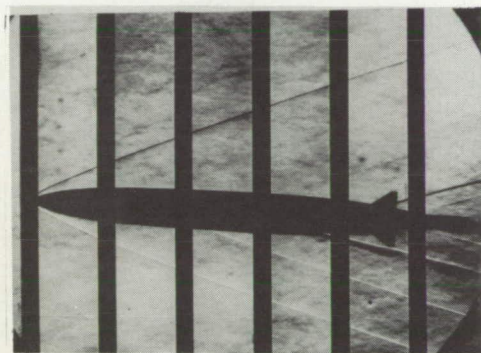




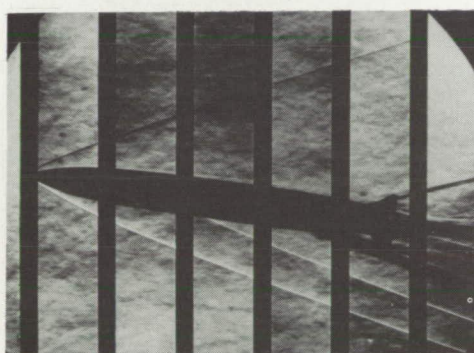
$\alpha = -4.1^\circ$



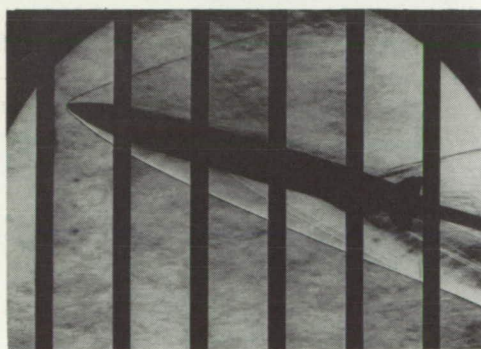
$\alpha = 0^\circ$



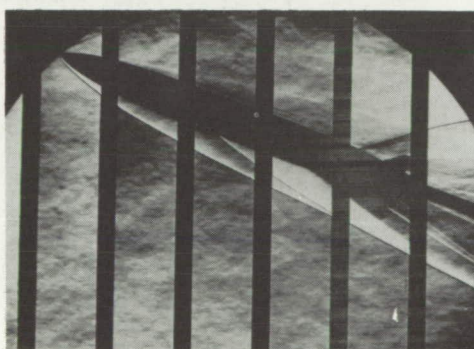
$\alpha = 4.2^\circ$



$\alpha = 8.3^\circ$



$\alpha = 17.0^\circ$



$\alpha = 21.1^\circ$

(c)  $M = 3.51$ .

L-58-160

Figure 4.- Concluded.



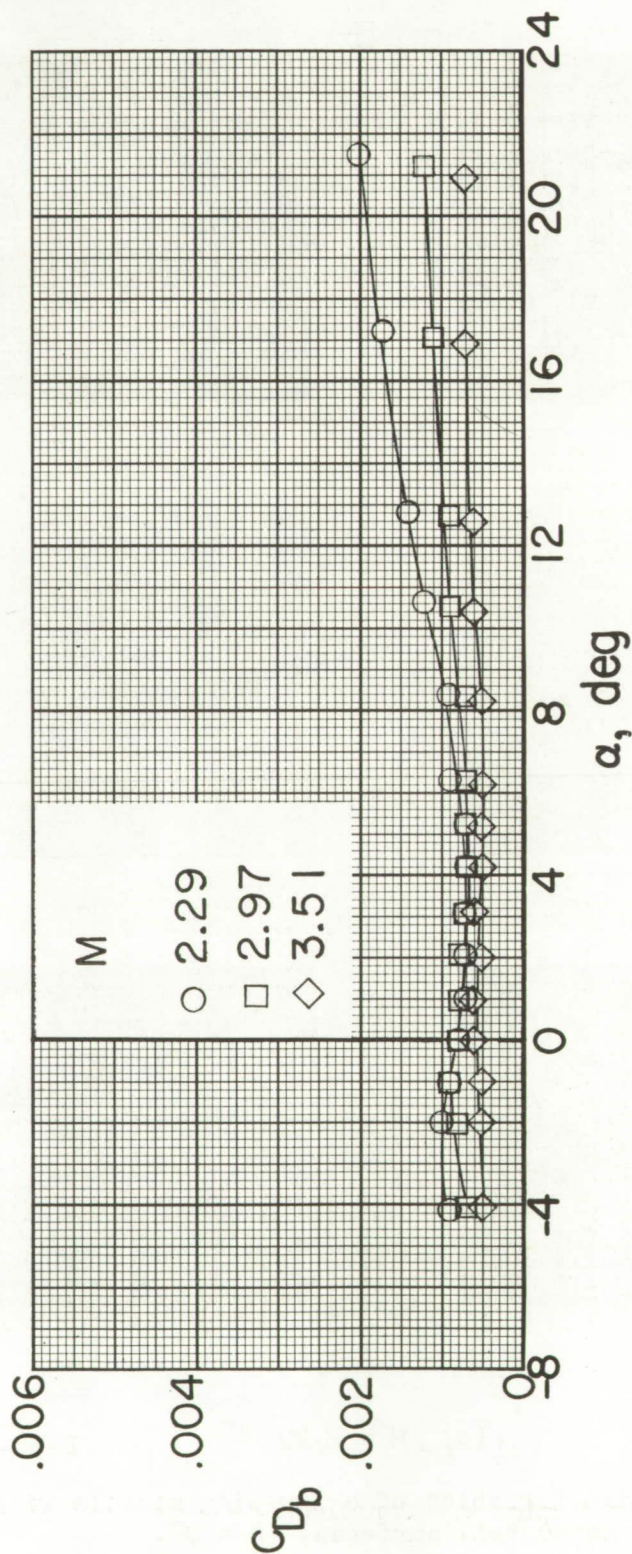
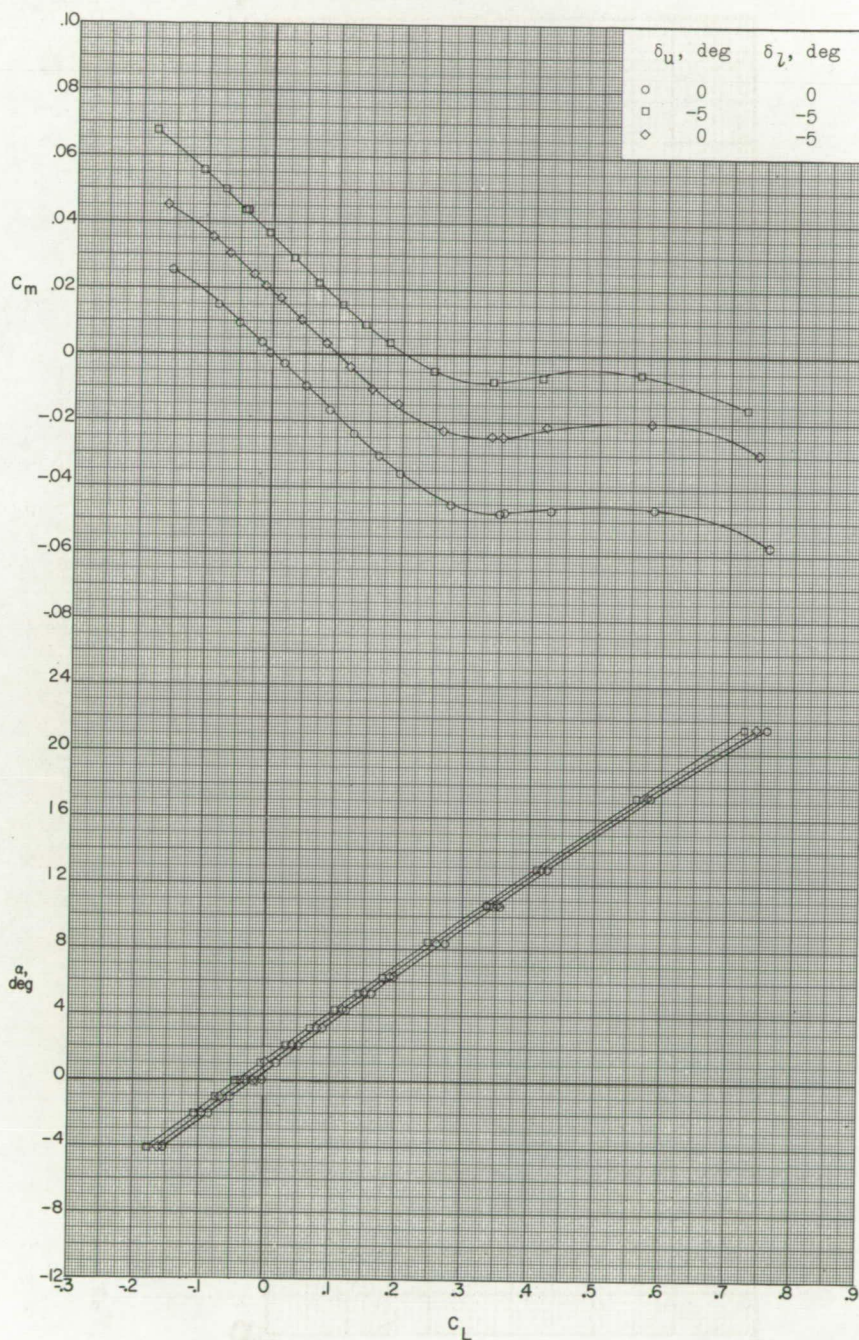


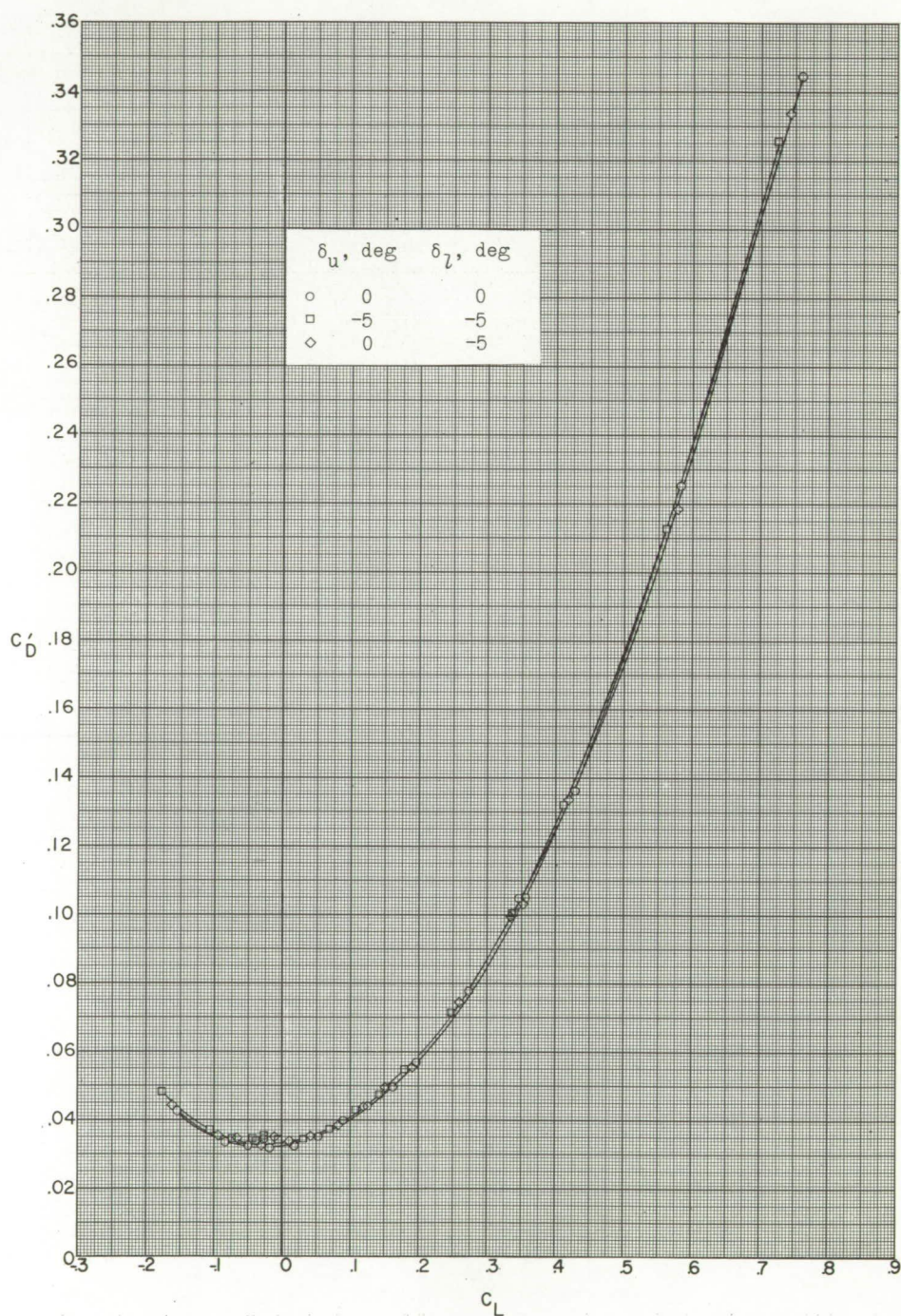
Figure 5.- Variation of base drag coefficient with angle of attack for a low-wing missile configuration with interdigitated tail surfaces.

CONFIDENTIAL

(a)  $M = 2.29$ .Figure 6.- Pitch characteristics of a low-wing missile with interdigitated tail surfaces.  $\beta = 0^\circ$ .

CONFIDENTIAL

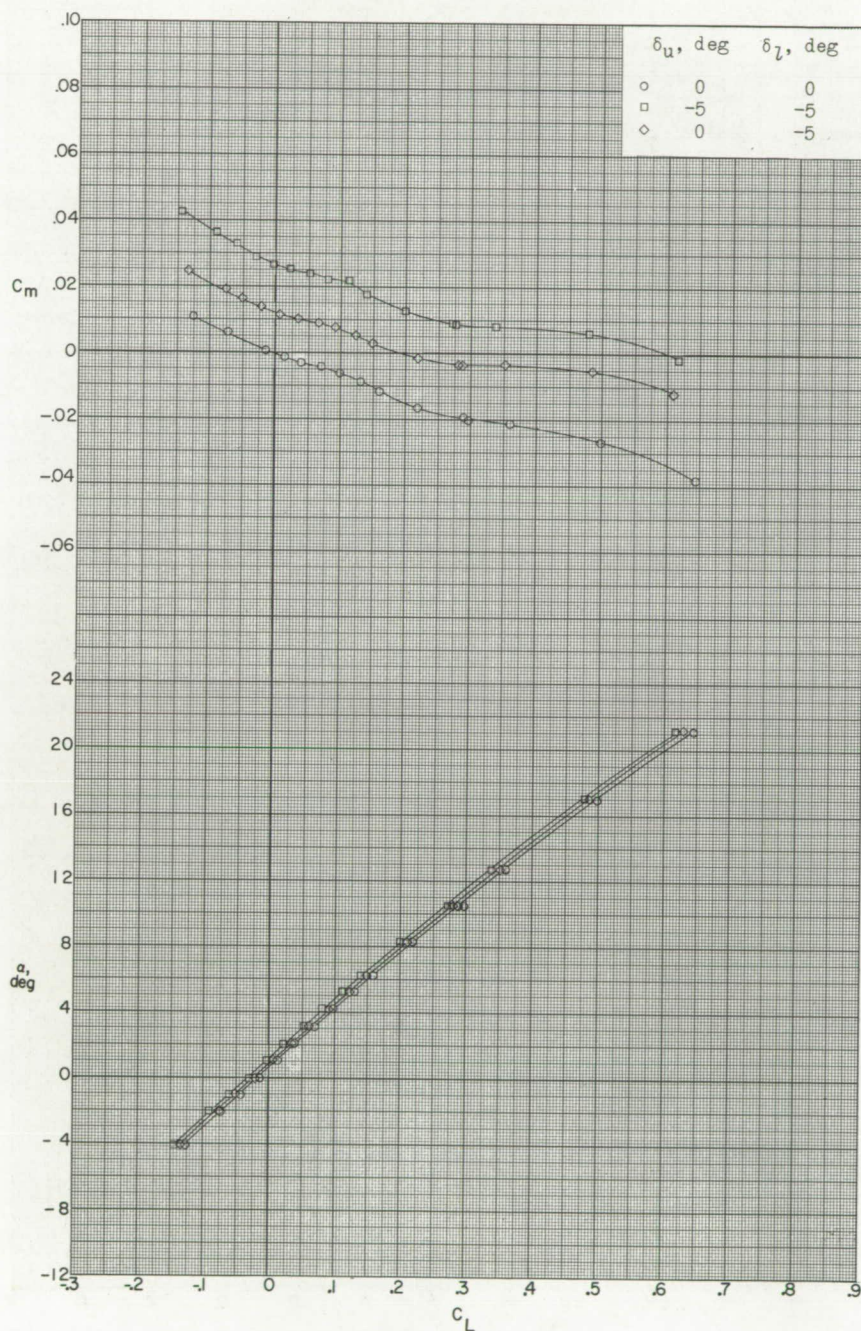




(a) Concluded.

Figure 6.- Continued.

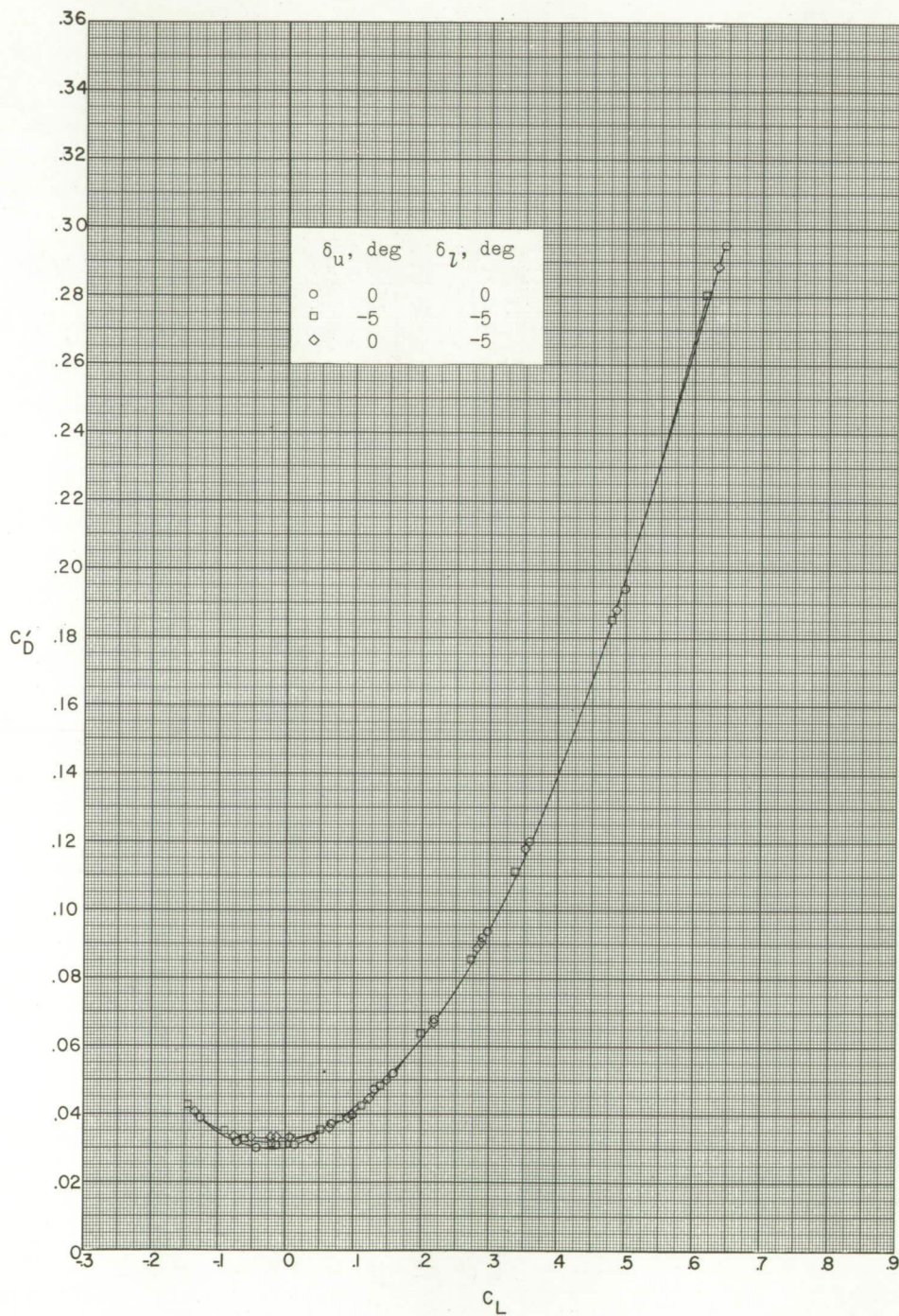




(b)  $M = 2.97$ .

Figure 6.- Continued.

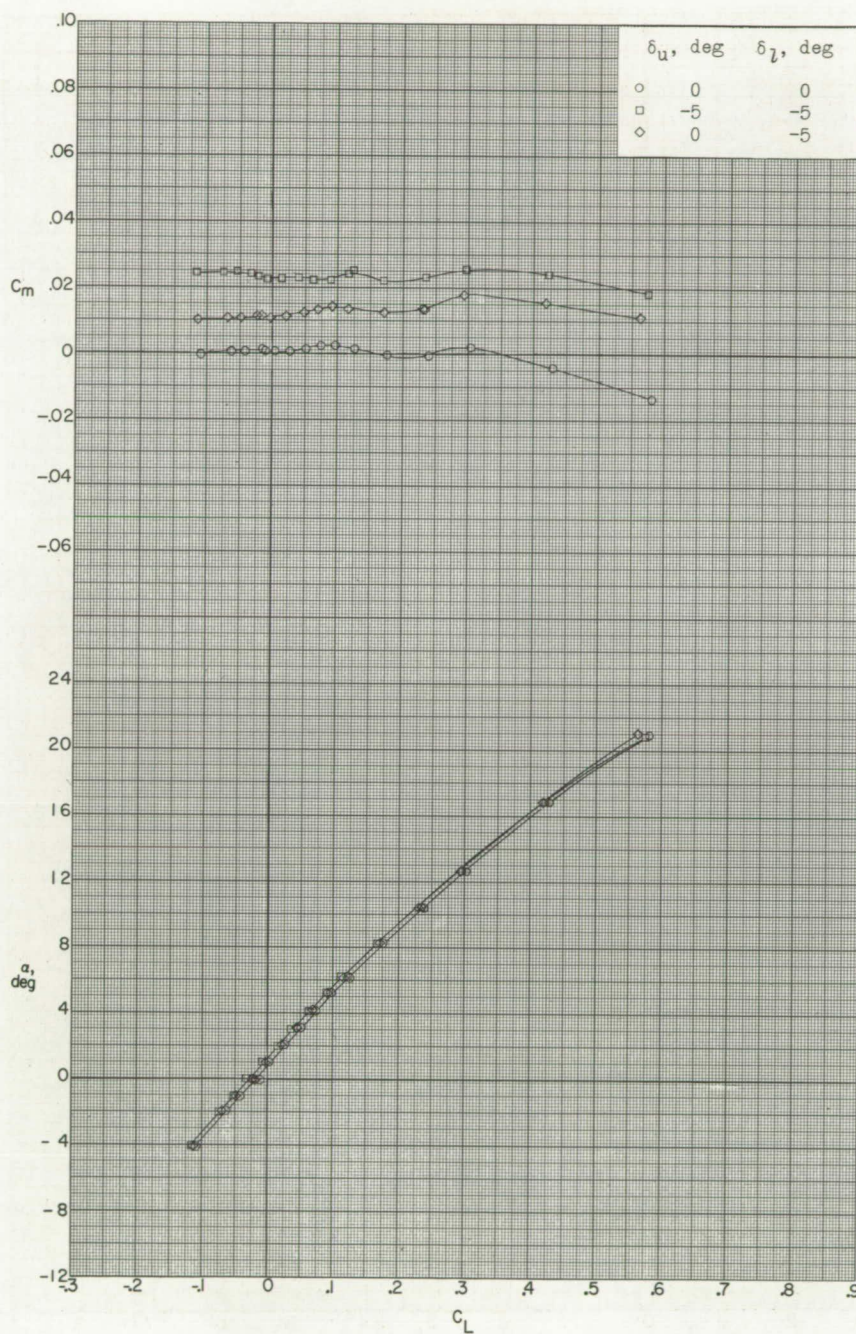




(b) Concluded.

Figure 6.- Continued.

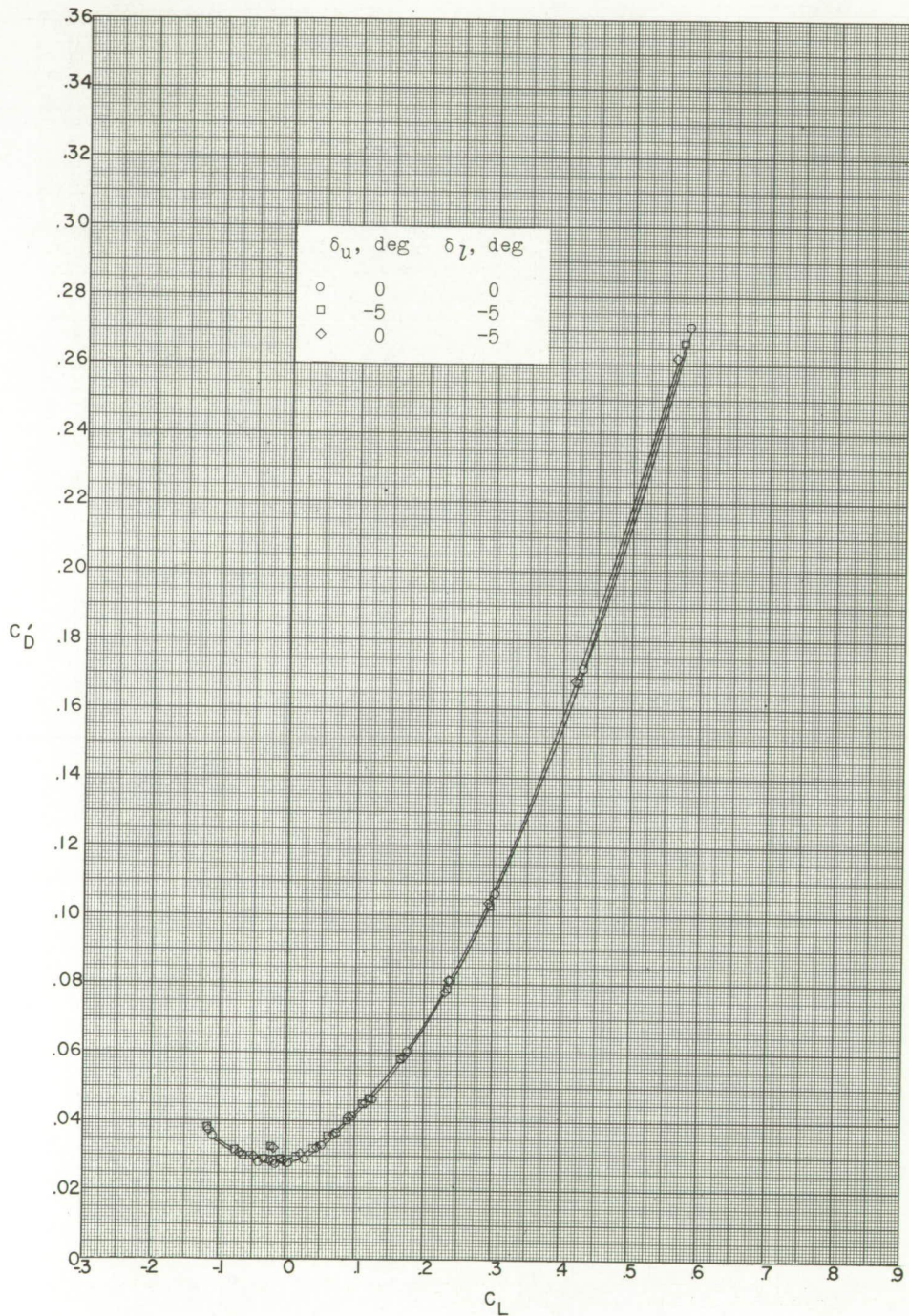




(c)  $M = 3.51$ .

Figure 6.- Continued.





(c) Concluded.

Figure 6.- Concluded.



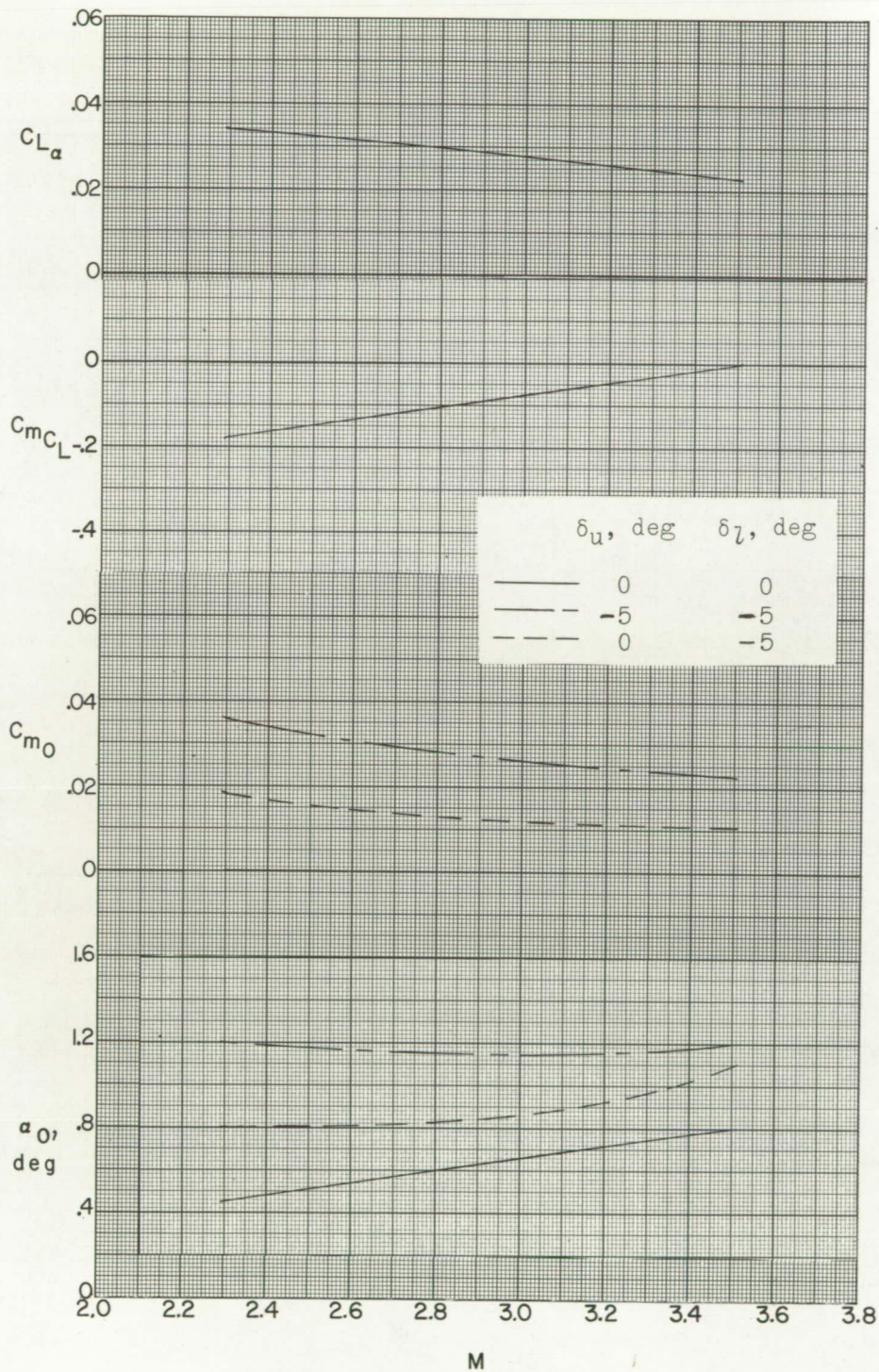


Figure 7.- Summary of the pitch characteristics of a low-wing missile with interdigitated tail surfaces.



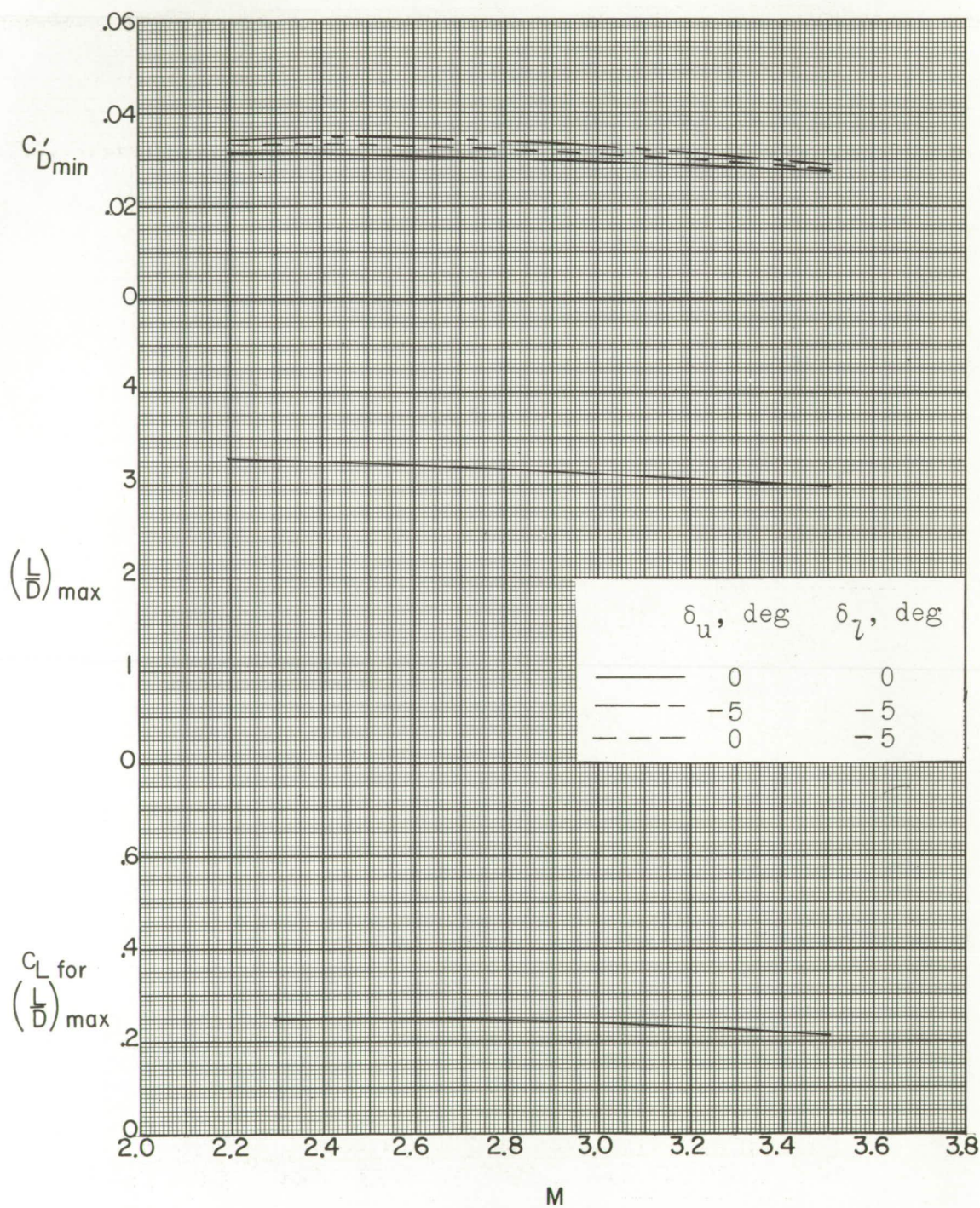


Figure 7.- Concluded.



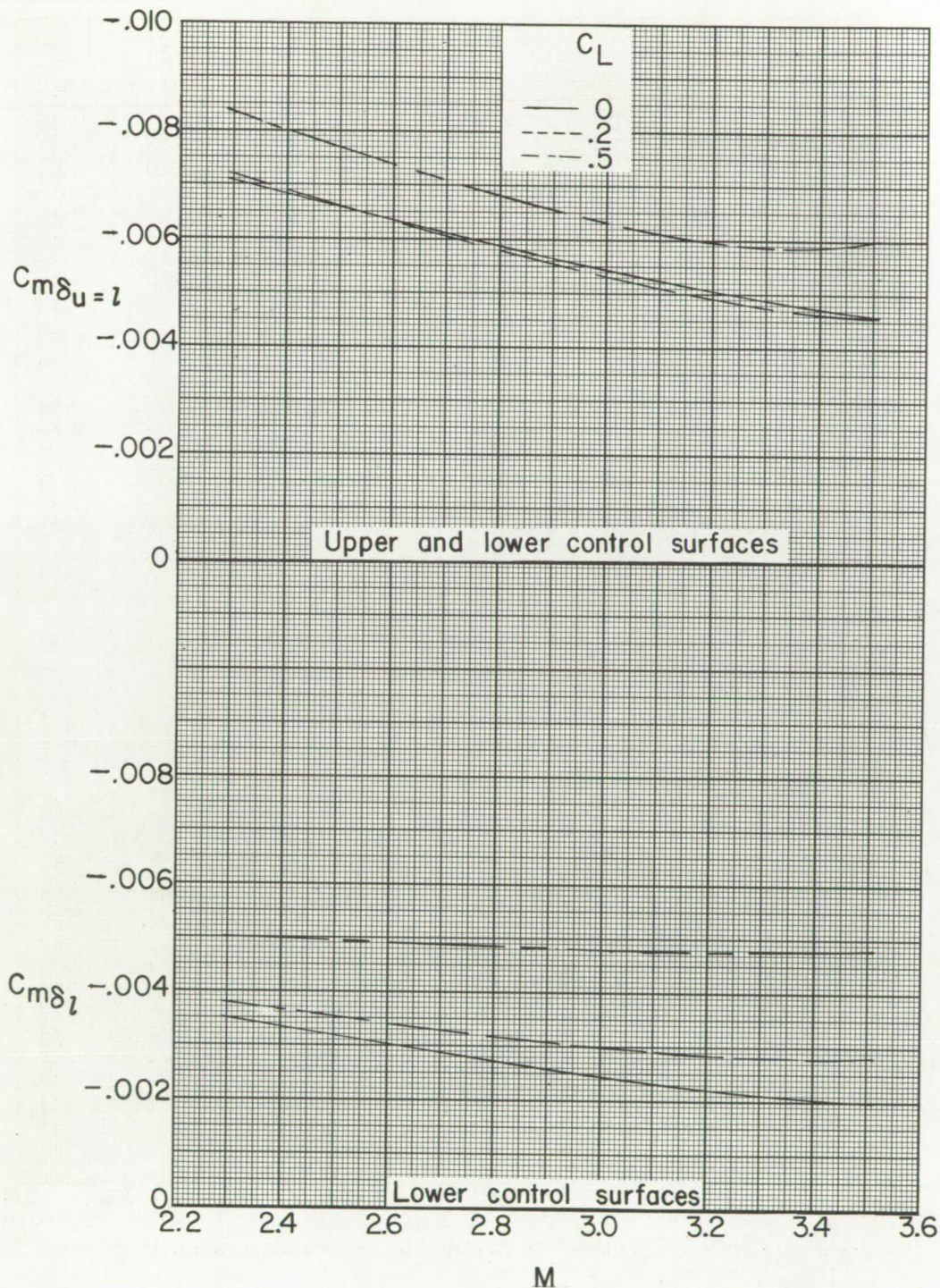


Figure 8.- Effect of lift coefficient on longitudinal control surface effectiveness of interdigitated tail surfaces on a low-wing missile.



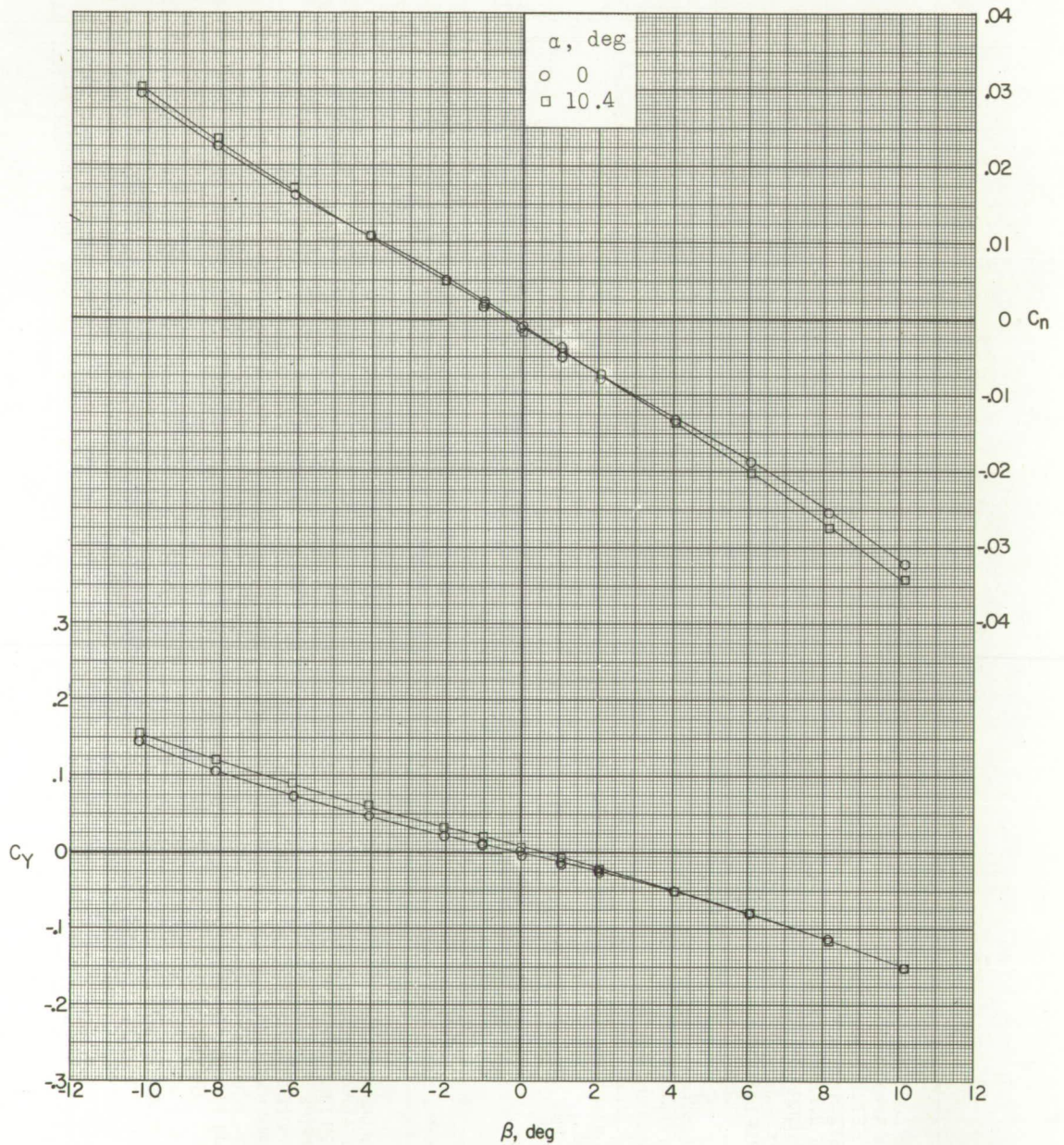


Figure 9.- Lateral characteristics of a low-wing missile with interdigitated tail surfaces (presented about the stability system of axes).  
 $M = 3.51$ ;  $\delta_{u=1} = 0^\circ$ .

03 7 15 4 10 00

CONFIDENTIAL